© 2018. Published by The Company of Biologists Ltd | Journal of Experimental Biology (2018) 221, jeb184564. doi:10.1242/jeb.184564

SHORT COMMUNICATION

Splitting of circulating red blood cells as an *in vivo* mechanism of erythrocyte maturation in developing zebrafish, chick and mouse embryos

Daniel Brönnimann[1], Tiziana Annese[1,2], Thomas A. Gorr[3,*] and Valentin Djonov[1,*,‡]

ABSTRACT

Nucleated circulating red blood cells (RBCs) of developing zebrafish, chick and mouse embryos can actively proliferate. While marrow- or organ-mediated erythropoiesis has been widely studied, transforming *in vivo* processes of circulating RBCs are under little scrutiny. We employed confocal, stereo- and electron microscopy to document the maturation of intravascular RBCs. In zebrafish embryos (32–72 h post-fertilization), RBC splitting in the caudal vein plexus follows a four-step program: (i) nuclear division with continued cytoplasmic connection between somata; (ii) dumbbell-shaped RBCs tangle at transluminal vascular pillars; (iii) elongation; and (iv) disruption of soma-to-soma connection. Dividing RBCs of chick embryos, however, retain the nucleus in one of their somata. Here, RBC splitting acts to pinch off portions of cytoplasm, organelles and ribosomes. Dumbbell-shaped primitive RBCs re-appeared as circulation constituents in mouse embryos. The splitting of circulating RBCs thus represents a biologically relevant mechanism of RBC division and maturation during early vertebrate ontogeny.

KEY WORDS: Erythropoiesis, Erythroblasts, Circulation, Vascular pillars, Shear stress

INTRODUCTION

From an evolutionary perspective, mammalian red blood cells (RBCs) are enucleated (Orkin and Zon, 1997) to increase hemoglobin levels (Ji et al., 2011). Because the committed production of the erythroid lineage via definitive erythropoiesis uniquely includes nuclear extrusion in mammals, the red cell population in the peripheral circulation of, say, adult rodents or humans consists entirely of nucleus-free erythrocytes. Nucleated and larger-sized RBCs, in contrast, are found in the peripheral blood of non-mammalian vertebrates such as birds (Schwartz and Stansbury, 1954) and teleost fish (Randall et al., 2014), as well as in prenatal vertebrate stages, including early mammalian embryos, as a result of primitive erythropoiesis.

Aside from murine models, the zebrafish is another lab species that is increasingly utilized in hematopoietic research because of its amenability to genetic manipulations and regenerative capacity (Hlushchuk et al., 2016; Poss et al., 2003). Primitive erythropoiesis in the zebrafish takes place in various regions, most prominently in the inner cell mass (Orkin and Zon, 2008). Once blood circulation starts at 24 h post-fertilization (hpf), primitive RBCs enter the bloodstream and mature (Kulkeaw and Sugiyama, 2012). It is thought that primitive erythropoiesis accounts for all circulating RBCs until 4 days post-fertilization (dpf) (Kulkeaw and Sugiyama, 2012). From 26 to 48 hpf, definitive hematopoietic precursors emerge from endothelial cells lining the ventral wall of the dorsal aorta. The space between the dorsal aorta and axial vein is equivalent to the aorta–gonad–mesonephros region of mouse ontogeny at embryonic days E10.5–E12.5. These definitive precursors progressively appear between 2 and 6 dpf in the circulation and subsequently expand within the caudal hematopoietic tissue of larval fish. Hematopoiesis of the adult fish shifts to the kidney marrow and thymus (Kulkeaw and Sugiyama, 2012).

In chick development, primitive hematopoiesis occurs in the blood islands of the yolk sac (Lassila et al., 1982). As a result, immature RBCs (erythroblasts) enter the circulation and undergo several mitoses along with their terminal differentiation (Baumann and Meuer, 1992). These yolk sac-derived primitive RBCs remain the principal red cell population until day 6 of embryonic development. By that time, definitive RBCs originate from stem cells located in the wall of the aorta and enter the vascular bed, thus gradually replacing primitive lineage constituents. Definitive RBCs are unable to produce embryonic hemoglobin; instead they mainly synthesize the two adult hemoglobins HbA and HbD (Baumann and Meuer, 1992).

In the mouse embryo, primitive erythroid cells, with their nucleated morphology and expression of embryonic plus adult hemoglobins (Kingsley et al., 2004), start developing in yolk sac blood islands between days 7 and 8 of embryonic development and, shortly thereafter, are seen circulating in the bloodstream until E16.5 (Baron et al., 2013; Fraser et al., 2007; Kingsley et al., 2004). From E9.5 to E12.5, the embryonic blood is dominated by large basophilic proerythroblasts, while during the 24 h period from E12.5 to E13.5 a striking change in Giemsa reactivity, illustrated by a switch to orthochromatophilic erythroblasts as the predominant erythroid entity, takes place (Fraser et al., 2007). Eventually, primitive mouse erythroblasts extrude their nuclei between E12.5 and E16.5 (Kingsley et al., 2004; McGrath et al., 2008). Definitive erythrocytes, with their smaller size, enucleated appearance and accumulation of adult, but not embryonic, hemoglobin originate in the fetal liver at E12.5 and rapidly predominate as circulating RBCs.

This is the first study documenting the tangling and splitting of circulating primitive RBCs as an *in vivo* mechanism for RBC division in zebrafish or mouse embryos and RBC maturation in chicken.

[1]University of Bern, Institute of Anatomy, Baltzerstrasse 2, 3012 Bern, Switzerland. [2]University of Bari Medical School, Department of Basic Medical Sciences, Neurosciences and Sensory Organs, Section of Human Anatomy and Histology, 70124 Bari, Italy. [3]University of Zurich, Institute of Veterinary Physiology, Vetsuisse Faculty, Winterthurerstrasse 260, 8057 Zurich, Switzerland.
*Co-senior authors

‡Author for correspondence (djonov@ana.unibe.ch)

D.B., 0000-0003-0476-2590; T.A., 0000-0002-7752-0368; T.A.G., 0000-0002-6023-4234; V.D., 0000-0003-0529-9665

Received 14 May 2018; Accepted 13 June 2018

MATERIALS AND METHODS

Confocal microscopy of zebrafish embryos

Zebrafish embryos, *Danio rerio* (F. Hamilton 1822), were dechorionated around 28 hpf and mounted in E3 medium (5 mmol l^{-1} NaCl, 0.17 mmol l^{-1} KCl, 0.33 mmol l^{-1} $CaCl_2$, 0.33 mmol l^{-1} $MgSO_4$) containing 0.4% low-melting point agarose, 0.003% phenylthiourea and 0.02% MS-222 (all reagents from Sigma-Aldrich, Buchs, Switzerland). Overnight imaging of several caudal vein plexus (CVP) regions was performed at 28.5°C using a Zeiss LSM880 confocal microscope with an LD C-apochromat 40×/1.1 W objective (Zeiss, Oberkochen, Germany). All images and videos were processed using Fiji v1.50i (Schindelin et al., 2012). To assess RBC mitosis, whole-mount immunohistochemistry using phospho-histone H3 (pH3) antibodies (Merck Millipore, Schaffhausen, Switzerland; Ref: 06-570) was performed with double-transgenic embryos *Tg(fli1a:GFP;gata1:DsRed)* at 48 hpf. Because of the presence of a *fli1a* promoter, these transgenics express a GFP reporter selectively in their vascular endothelial cells (green fluorescing vascular network), while erythroid precursors and RBCs are highlighted *in vivo* through expression of a DsRed fluorophore under the control of the *gata1* promoter (see Fig. 1). Our zebrafish experiments were ethically approved by the Cantonal Veterinary Office (license number: BE59/15; validity: 31 October 2018).

Chicken chorioallantoic membrane (CAM) assay

Chicken embryos, *Gallus gallus domesticus* (Linnaeus 1758), were pre-incubated at 37°C and placed in 100×20 mm Petri dishes (Corning, NY, USA) at post-incubation day 3. At day 7 (n=3), day 10 (n=5) and day 13 (n=3), 100 µl of 10% FITC-dextran (2 MDa; Sigma-Aldrich) was injected below the CAM for contrast enhancement. Images and videos were acquired using a Leica DFC365X camera mounted on a Leica stereomicroscope M205FA (Leica Microsystems, Heerbrugg, Switzerland). Blood smears were stained with Giemsa May–Grünwald (Sigma-Aldrich) on day 5 (n=4), day 7 (n=6), day 10 (n=7) and day 13 (n=2). For transmission electron microscopy, blood was collected on day 10 (n=4), centrifuged (1000 rpm, 4 min) in 2.5% glutaraldehyde (540 mOsm, pH 7.4) and post-fixed in osmium tetroxide (340 mOsm, pH 7.4). Next, samples were embedded in epon812 and stained using uranyl acetate and lead citrate. For the time period used herein (day 7–day 13), CAM assays are not considered animal tests by Swiss legislature.

Blood samples from mouse embryos

Six to 12 mouse embryos, *Mus musculus* Linnaeus 1758, were harvested from gravid C57BL/6JRj females killed by cervical dislocation at developmental days E9.5, E11, E12.5 and E14. Smears of embryonic blood from any of these stages were prepared, mitotic figures of cells were stained with Giemsa May–Grünwald and images were documented using a Zeiss Axio Imager M2 light microscope (Zeiss) with an Olympus UC50 color-CCD camera (Olympus Schweiz AG, Volketswil, Switzerland). The mitotic frequency of primitive RBCs as proportion of 1000 counted erythroid cells was determined per developmental stage in comparison with maternal blood by five different individuals through manual counting. Evidence for *in vivo* mitosis and dumbbell morphology of nucleated primitive RBCs was obtained using whole-mount preparations of embryonic yolk sacs and umbilical cord tissue. Following fixation of the tissue in Karnovsky buffer (2.5% glutaraldehyde + 2% paraformaldehyde in 0.1 mol l^{-1} cacodylate buffer, pH 7.4), cells were DAPI stained and visualized in a Zeiss LSM880 confocal microscope with a Plan Apochromat 63×/1.4 NA oil objective (Zeiss). The mouse experiments were ethically approved by the Cantonal Veterinary Office (license number: BE43/18; validity: 01 June 2020).

Statistical analyses

All statistical analyses were performed with GraphPad Prism v5.04. P-values of two-tailed paired t-tests were considered statistically significant if $P<0.05$ ($*P<0.05$, $**P<0.01$, $***P<0.001$). Values are given as means±95% confidence interval.

RESULTS AND DISCUSSION

RBC splitting as a biologically relevant mechanism of RBC division during zebrafish development

Blood is a major site of erythrocyte proliferation and maturation in lower vertebrates and early ontogenic stages. Yamamoto and Iuchi (1975) were, to the best of our knowledge, the first to demonstrate by electron microscopy the maturation of primitive erythroid cells in the circulation of rainbow trout embryos. Although later studies pointed to the importance of mitoses to promote the maturation of circulating RBCs in fish (Glomski et al., 1992), further mechanistic insights into molecular or biomechanical cues to initiate and govern both proliferation and maturation of red cells in the bloodstream were slow to emerge. Here, we demonstrate for the first time that splitting of circulating RBCs marks a quantitatively meaningful *in vivo* mechanism of RBC division in zebrafish embryos and that vascular bifurcations and transluminal pillars are key biomechanical components in triggering the process.

Between 28 and 72 hpf, the CVP (Isogai et al., 2001) of zebrafish embryos consists of a highly interconnected vascular network (Fig. 1A,B; Movie 1). RBC splitting in the CVP proceeds as a four-step process (Movie 2). (i) Division: mitotic activity of circulating RBCs was determined using whole-mount pH3 staining of 48 hpf *Tg(fli1a:GFP;gata1:DsRed)* zebrafish (Fig. 1B,C). *Gata1* is a marker for red blood cells and erythroid precursors (Traver et al., 2003). On average, 1.49±0.28% (n=9) of the intravascular *gata1*$^+$ cells in the CVP were pH3$^+$ (Fig. 1D). (ii) Tangling: long-term confocal imaging of the CVP was performed between 36 and 72 hpf. On average, 11.24±0.93 (n=11) dumbbell-shaped RBCs tangled up per hour at vascular bifurcations and transluminal pillars, per region (Fig. 1F). We identified around 3–4 tangling regions per embryo, suggesting ∼1000 splitting events occur per day between 32 and 72 hpf. This high frequency would render RBC splitting a biologically meaningful mechanism for RBC division. (iii) Elongation: once tangled, RBCs remained at the vascular structure where the soma-to-soma connection subsequently elongated (Fig. 1E). Afterwards, elongation proceeded by exponential growth, indicating the process occurs faster with longer-lasting tangles (Fig. 2E,F). Tangled RBCs receive constant blood flow with strong shear forces as potent morphogenic cues, which are known to regulate a variety of processes (Brönnimann et al., 2016; Hoefer et al., 2013; North et al., 2009). However, elevated blood flow velocity, a key determinant of shear forces, altered neither splitting time nor elongation speed, suggesting that RBC splitting itself is unaffected by incident shear stress (Fig. 2A–D). (iv) Splitting: after 129.56±1.29 s (n=11), the connection between the somata eventually broke, thus releasing two separate cell bodies into circulation (Fig. 1G).

RBC splitting contributes to RBC maturation during chick development

To assess whether RBC splitting adds to the renewal of nucleated RBCs in other models, we utilized the chick CAM with its dense

Journal of Experimental Biology (2018) 221, jeb184564. doi:10.1242/jeb.184564

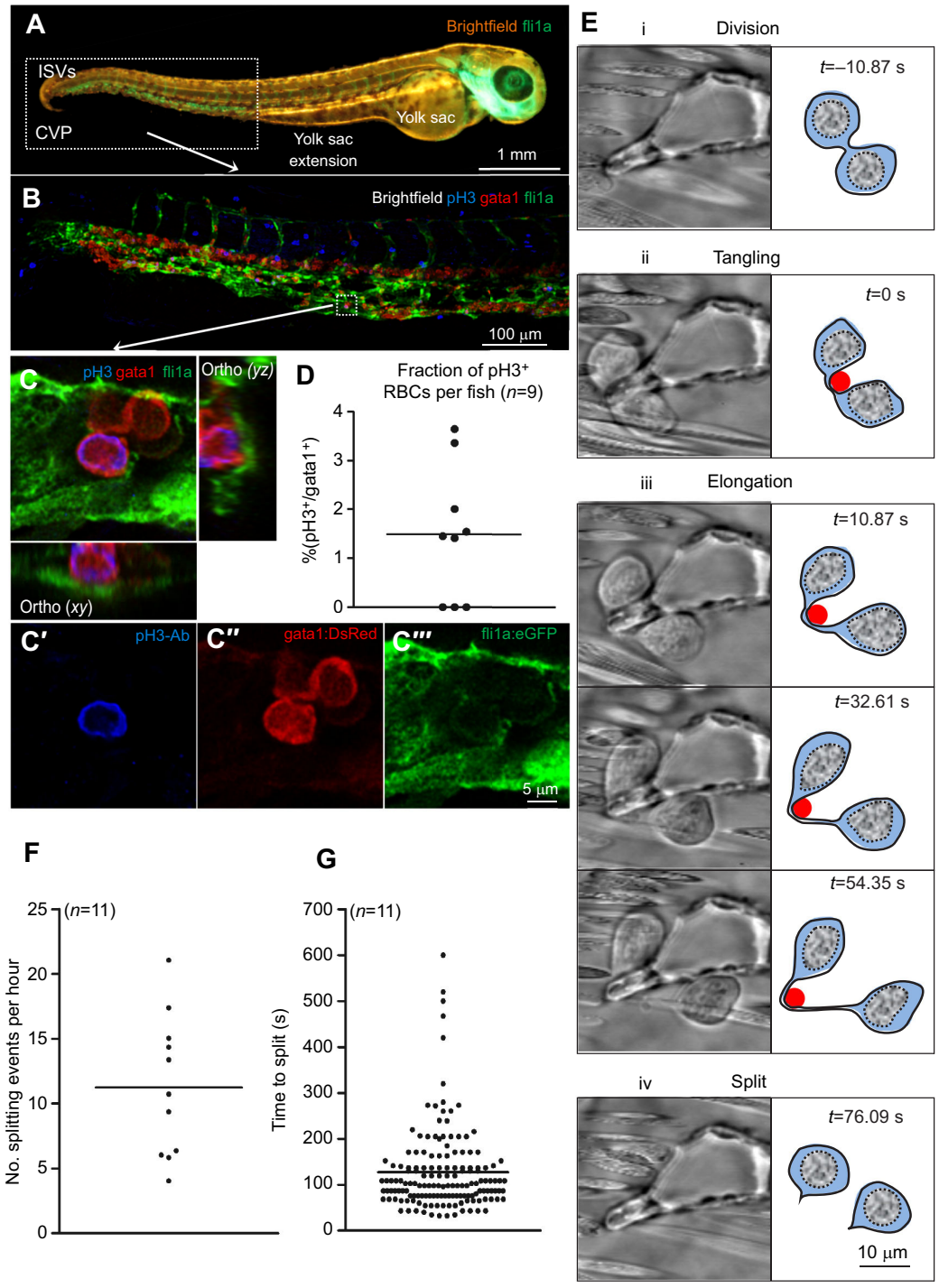

Fig. 1. *In vivo* proliferation and splitting of circulating red blood cells (RBCs) in zebrafish embryos. (A) Overview of a zebrafish embryo at 48 hours post-fertilization (hpf) *in vivo*. ISVs, intersegmental vessels; CVP, caudal vein plexus. (B) Phospho-histone H3 (pH3) staining (blue) of the zebrafish caudal vein plexus. In *Tg(fli1a:GFP;gata1:DsRed)* double transgenic animals, endothelial cells (green) and RBCs (red) are labeled through expression of fluorescent markers as indicated. (C) Example of a pH3-positive circulating RBC. (D) Average extent of pH3-positive cells as percentage of circulating *gata1*-positive RBCs (n=9; >100 quantified RBCs per animal). (E) Splitting of proliferating RBCs is a four-step process. Following cell division (i), the two somata of a dividing RBC might eventually tangle (ii) at a vascular bifurcation which leads to the subsequent elongation (iii) of the soma-to-soma connection and its eventual rupture (iv). (F) We observed 11.24±0.93 RBC splitting events per hour (n=11; 142 events in total). (G) On average, a splitting event (i.e. phase ii–iv) occurred within 129.56±1.29 s (n=11; 142 events).

Journal of Experimental Biology (2018) 221, jeb184564. doi:10.1242/jeb.184564

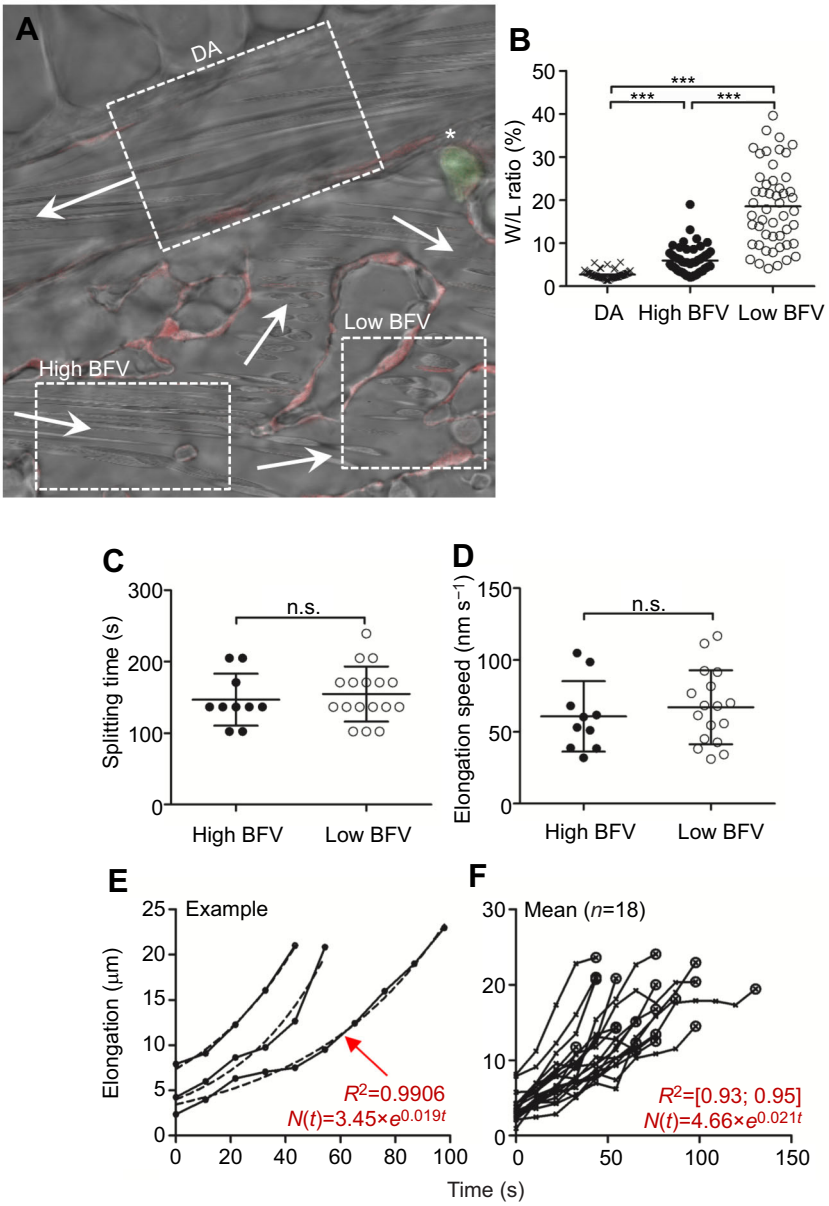

Fig. 2. RBC splitting is independent of the incident blood flow velocity in zebrafish embryos *in vivo*. To assess the impact of blood flow velocity (BFV) as a major shear force determinant on splitting time and elongation speed during RBC splitting, we compared RBC splitting at two regions receiving either high or low BFV. (A) Three regions in a *Tg(fli1a:RedX;mpx:eGFP)* fish, the dorsal aorta (DA), high BFV and low BFV, are indicated. Arrows mark the respective blood flow direction. The asterisk indicates a primitive neutrophil. (B) BFV was deduced by the width/length (W/L) ratio of adjacent circulating blood cells. Images were acquired throughout a constant period of time. In regions with high BFV (i.e. DA), RBCs are elongated (i.e. L>W, low W/L ratio), while at low BFV, RBCs appear more rounded (i.e. increased W/L ratio). Therefore, the W/L ratio serves as a proxy for the local BFV. ***P<0.001. (C) Splitting time and (D) elongation speed were both independent on BFV. (E,F) Exponential growth (E) and elongation length (F). Once RBCs are tangled at vascular structures (phase ii), the soma-to-soma connection subsequently elongates (phase iii). The process of elongation can be mathematically expressed using exponential growth equations. This implies that the longer a cell is tangled, the faster its retained connection elongates. On average, elongation was represented by the equation $N(t)$=4.66×e0.021t with a regression coefficient (R^2) between 0.93 and 0.95 (n=1 animal, n=18 events).

capillary plexus forming around day 10 (Djonov et al., 2000; Ribatti et al., 2001). Contrary to our findings with zebrafish embryos, we observed thousands of simultaneous tangling events in the CAM (Fig. 3A,B; Movie 3). In blood smears (Fig. 3C,D), the fraction of immature RBCs with mitotic figures decreased dramatically between day 7 (8.48±1.39%) and day 10 (0.19±0.1%; P=0.0013) (Fig. 3E). Pre- and post-tangling RBCs were present only after day 7. After day 7, immature RBCs polarize and become dumbbell-shaped structures (Fig. 3D), with the nucleated soma and the non-nucleated appendix remaining connected by a weakly labeled cytoplasmic bridge. The frequent occurrence of post-tangle figures in the blood at day 10 and day 13 strongly suggests RBC splitting (Fig. 3D), although we were unable to document an entire event *in vivo*. Possibly, chick elongation phases markedly exceed those in zebrafish.

Recruitment of erythroblasts from extravascular yolk sac sites along with mitotic maturation plus terminal differentiation of primitive RBCs inside the circulation of the chicken embryo have already been reported (Baumann and Meuer, 1992). Immature avian and zebrafish RBCs contain functional mitochondria and numerous free ribosomes for protein synthesis (Moritz et al., 1997). From the differentiation of basophilic erythroblasts to polychromaphilic erythroblasts and mature RBCs, the amount of free ribosomes progressively decreases (Brasch et al., 1974; Glomski and Pica, 2011). Consequently, protein synthesis and mitochondrial oxygen consumption slow down, which effectively decreases reactive oxygen species production and increases oxygen availability (Stier et al., 2013; Zhang et al., 2011). In electron micrographs, immature (pre-tangle) RBCs displayed higher ribosomal and mitochondrial content than mature (post-tangle) RBCs (Fig. S1a–d), suggesting that RBC splitting underlies the reduction of ribosome numbers, mitochondria and possibly other organelles in chick RBCs undergoing maturation.

RBC splitting promotes the division of circulating primitive RBCs in mouse embryos

Abundant evidence for the division of circulating nucleated RBCs, including dumbbell-shaped daughter cells that retained a

Journal of Experimental Biology (2018) 221, jeb184564. doi:10.1242/jeb.184564

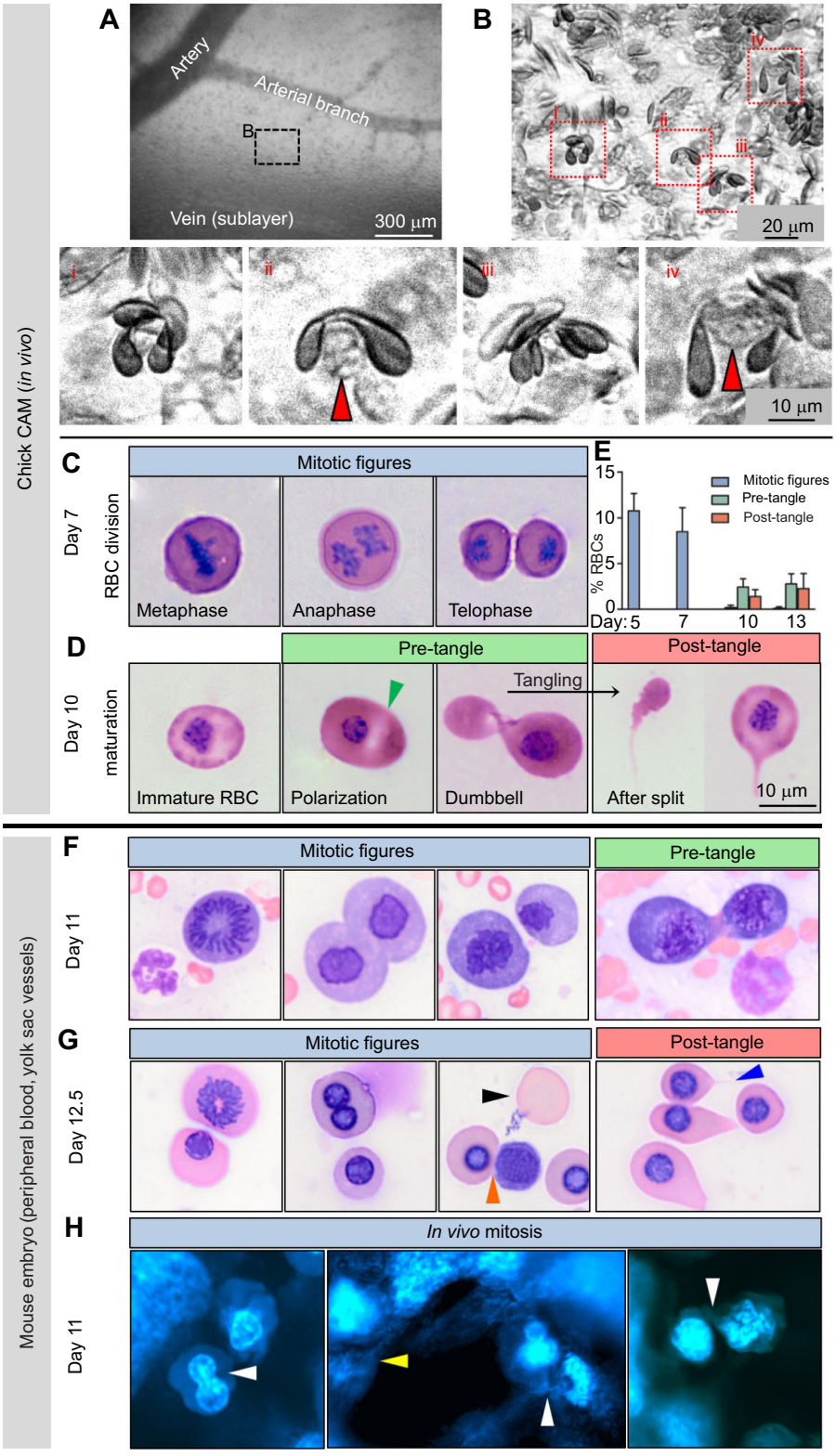

Fig. 3. RBC splitting promotes RBC maturation in the chick embryo and division of circulating primitive RBCs in the mouse embryo. (A–E) Chick embryo; (F–H) mouse embryo. (A) Overview of the vascular network in the chick chorioallantoic membrane (CAM) with indicated arteries and veins. (B) Capillary network and (i–iv) examples of tangled RBCs. RBCs tangle at transluminal pillars (red arrowheads). (C) Blood smears of isolated chick blood at day 7 show mitotically active RBCs. (D) At day 10, immature RBCs undergo polarization. The nucleus is transferred opposite to a strongly azurophilic region and both are separated by a weakly labeled region (green arrowhead). Thereafter, RBCs become dumbbell shaped, tangle at vascular structures and eventually release nucleated and non-nucleated somata into the peripheral blood. (E) Quantification of mitotically active, pre-tangle and post-tangle RBCs in the blood smear (see Results and Discussion). (F,G) Examples of mitotic (E11, E12.5) and pre- (E11) and post-tangled (E12.5) figures in blood smears taken from mouse embryos at the indicated developmental stages. Small, pink-colored RBCs without a nucleus (particularly at E11) derive from contaminating maternal blood. During the time span E9.5–E12.5 of mouse ontogeny, the embryonic blood is dominated by large basophilic proerythroblasts (i.e. day 11), while during the 24 h period from E12.5 to E13.5, a striking change in Giemsa reactivity, illustrated by a switch to orthochromatophilic erythroblasts as the predominant erythroid entity, takes place (i.e. day 12.5) (Fraser et al., 2007). Black arrowhead: enucleated primitive RBC. Orange arrowhead: example of post-mitotic cell doublet, not uncommon at E12.5, with one daughter cell of basophilic and the other of orthochromatophilic Giemsa reactivity. Blue arrowhead: post-tangle cytoplasmic protrusions. (H) *In vivo* mitosis in umbilical vessels of E11 mouse embryo yolk sacs. Dark channels illustrate the lumen of vessels. Left image: example of intra-luminal mitosis of a nucleated DAPI-stained murine erythroblast (white arrowhead). Central image: example of the dumbbell structure of two nucleated RBC daughter cells, still retaining the cytoplasmic bridge between somata (white arrowhead). In close proximity, one notices thin fibers spanning from one side of the vascular wall to the opposite side (yellow arrowhead). Right image: example of the intra-luminal dumbbell structure of two nucleated RBC daughter cells, almost completely separated (white arrowhead points to the thin cytoplasmic junction).

cytoplasmic bridge between two nucleated somata, was also obtained in Giemsa-stained blood smears from E9.5-, E11- (Fig. 3F), E12.5- (Fig. 3G) and E14-staged embryos of C57BL/6JRj mice. The frequency of mitotic events ranged from 2.7% (E.9.5) to 3.5% (E14), without varying significantly between developmental stages (data not shown). As E12.5 embryos contain a total of 4.8 million Coulter-counted circulating RBCs (Kingsley et al., 2004), the mean 2.9% proportion of dividing cells obtained here amounts to a total of ∼139,000 mitotic cells within the peripheral blood of these embryos. Assuming a doubling time of approximately 8 h for primitive E12.5 RBCs (Isern et al., 2011), the 2.9% mitotic frequency yields an estimated daily renewal of a

considerable proportion (1.1 million or ∼23%) of the total population of circulating RBCs in E12.5 mouse embryos. DAPI staining of nucleated RBCs in conjunction with confocal microscopy allowed us to detect dividing RBCs and post-tangled dumbbell figures of RBCs within the umbilical vascular network of the embryonic yolk sac (Fig. 3H).

Collectively, RBC splitting was shown to underlie and promote the division of circulating RBCs in zebrafish and mouse embryos and the maturation of immature RBCs in the developing chick embryo.

Acknowledgements
Microscopy was performed on equipment supported by the Microscopy Imaging Center (MIC), University of Bern, Switzerland. The work was carried out during study or qualification programs of the (i) University of Bari: Transplantation of organs and tissues and cell therapies; and (ii) University of Bern: (a) Graduate School for Cellular and Biomedical Sciences; (b) BNF National qualification programme. The authors thank Prof. Nadia Mercader Huber for antibodies and fruitful discussions, Dr Roman Schönauer for help with confocal microscopy, Jeannine Wagner and Werner Graber for support in electron microscopy, and Regula Bürgy, Eveline Yao and Séverin Yao for their cell staining and cell counting assistance.

Competing interests
The authors declare no competing or financial interests.

Author contributions
Conceptualization: V.D.; Formal analysis: D.B., T.A., T.A.G.; Investigation: D.B., T.A., T.A.G., V.D.; Resources: V.D.; Data curation: D.B., T.A.G.; Writing - original draft: D.B.; Writing - review & editing: T.A.G., V.D.; Visualization: D.B., T.A.; Supervision: V.D.; Project administration: V.D.; Funding acquisition: V.D.

Funding
This work was supported by the Swiss National Foundation Grant no. CRSII3_154499/1 to V.D.

Supplementary information
Supplementary information available online at
http://jeb.biologists.org/lookup/doi/10.1242/jeb.184564.supplemental

References
Baron, M. H., Vacaru, A. and Nieves, J. (2013). Erythroid development in the mammalian embryo. *Blood Cells Mol. Dis.* **51**, 213-219.
Baumann, R. and Meuer, H. J. (1992). Blood oxygen transport in the early avian embryo. *Physiol. Rev.* **72**, 941-965.
Brasch, K., Adams, G. H. and Neelin, J. M. (1974). Evidence for erythrocyte-specific histone modification and structural changes in chromatin during goose erythrocyte maturation. *J. Cell Sci.* **15**, 659-677.
Brönnimann, D., Djukic, T., Triet, R., Dellenbach, C., Saveljic, I., Rieger, M., Rohr, S., Filipovic, N. and Djonov, V. (2016). Pharmacological modulation of hemodynamics in adult zebrafish in vivo. *PLoS ONE* **11**, e0150948.
Djonov, V. G., Galli, A. B. and Burri, P. H. (2000). Intussusceptive arborization contributes to vascular tree formation in the chick chorio-allantoic membrane. *Anat. Embryol.* **202**, 347-357.
Fraser, S. T., Isern, J. and Baron, M. H. (2007). Maturation and enucleation of primitive erythroblasts during mouse embryogenesis is accompanied by changes in cell-surface antigen expression. *Blood* **109**, 343-352.
Glomski, C. A. and Pica, A. (2011). *The Avian Erythrocyte: Its Phylogenetic Odyssey*. Boca Raton, FL, USA: CRC Press.
Glomski, C. A., Tamburlin, J. and Chainani, M. (1992). The phylogenetic odyssey of the erythrocyte. III. Fish, the lower vertebrate experience. *Histol. Histopathol.* **7**, 501-528.
Hlushchuk, R., Brönnimann, D., Correa Shokiche, C., Schaad, L., Triet, R., Jazwinska, A., Tschanz, S. A. and Djonov, V. (2016). Zebrafish caudal fin angiogenesis assay-advanced quantitative assessment including 3-way correlative microscopy. *PLoS ONE* **11**, e0149281.
Hoefer, I. E., den Adel, B. and Daemen, M. J. A. P. (2013). Biomechanical factors as triggers of vascular growth. *Cardiovasc. Res.* **99**, 276-283.
Isern, J., He, Z., Fraser, S. T., Nowotschin, S., Ferrer-Vaquer, A., Moore, R., Hadjantonakis, A.-K., Schulz, V., Tuck, D., Gallagher, P. G. et al. (2011). Single-lineage transcriptome analysis reveals key regulatory pathways in primitive erythroid progenitors in the mouse embryo. *Blood* **117**, 4924-4934.
Isogai, S., Horiguchi, M. and Weinstein, B. M. (2001). The vascular anatomy of the developing zebrafish: an atlas of embryonic and early larval development. *Dev. Biol.* **230**, 278-301.
Ji, P., Murata-Hori, M. and Lodish, H. F. (2011). Formation of mammalian erythrocytes: chromatin condensation and enucleation. *Trends Cell Biol.* **21**, 409-415.
Kingsley, P. D., Malik, J., Fantauzzo, K. A. and Palis, J. (2004). Yolk sac-derived primitive erythroblasts enucleate during mammalian embryogenesis. *Blood* **104**, 19-25.
Kulkeaw, K. and Sugiyama, D. (2012). Zebrafish erythropoiesis and the utility of fish as models of anemia. *Stem Cell Res. Ther.* **3**, 55.
Lassila, O., Martin, C., Toivanen, P. and Dieterlen-Lievre, F. (1982). Erythropoiesis and lymphopoiesis in the chick yolk-sac-embryo chimeras: contribution of yolk sac and intraembryonic stem cells. *Blood* **59**, 377-381.
McGrath, K. E., Kingsley, P. D., Koniski, A. D., Porter, R. L., Bushnell, T. P. and Palis, J. (2008). Enucleation of primitive erythroid cells generates a transient population of “pyrenocytes” in the mammalian fetus. *Blood* **111**, 2409-2417.
Moritz, K. M., Lim, G. B. and Wintour, E. M. (1997). Developmental regulation of erythropoietin and erythropoiesis. *Am. J. Physiol.* **273**, R1829-R1844.
North, T. E., Goessling, W., Peeters, M., Li, P., Ceol, C., Lord, A. M., Weber, G. J., Harris, J., Cutting, C. C., Huang, P. et al. (2009). Hematopoietic stem cell development is dependent on blood flow. *Cell* **137**, 736-748.
Orkin, S. H. and Zon, L. I. (1997). Genetics of erythropoiesis: induced mutations in mice and zebrafish. *Annu. Rev. Genet.* **31**, 33-60.
Orkin, S. H. and Zon, L. I. (2008). Hematopoiesis: an evolving paradigm for stem cell biology. *Cell* **132**, 631-644.
Poss, K. D., Keating, M. T. and Nechiporuk, A. (2003). Tales of regeneration in zebrafish. *Dev. Dyn.* **226**, 202-210.
Randall, D. J., Rummer, J. L., Wilson, J. M., Wang, S. and Brauner, C. J. (2014). A unique mode of tissue oxygenation and the adaptive radiation of teleost fishes. *J. Exp. Biol.* **217**, 1205-1214.
Ribatti, D., Nico, B., Vacca, A., Roncali, L., Burri, P. H. and Djonov, V. (2001). Chorioallantoic membrane capillary bed: a useful target for studying angiogenesis and anti-angiogenesis in vivo. *Anat. Rec.* **264**, 317-324.
Schindelin, J., Arganda-Carreras, I., Frise, E., Kaynig, V., Longair, M., Pietzsch, T., Preibisch, S., Rueden, C., Saalfeld, S., Schmid, B. et al. (2012). Fiji: an open-source platform for biological-image analysis. *Nat. Methods* **9**, 676-682.
Schwartz, S. O. and Stansbury, F. (1954). Significance of nucleated red blood cells in peripheral blood; analysis of 1,496 cases. *J. Am. Med. Assoc.* **154**, 1339-1340.
Stier, A., Bize, P., Schull, Q., Zoll, J., Singh, F., Geny, B., Gros, F., Royer, C., Massemin, S. and Criscuolo, F. (2013). Avian erythrocytes have functional mitochondria, opening novel perspectives for birds as animal models in the study of ageing. *Front. Zool.* **10**, 33.
Traver, D., Paw, B. H., Poss, K. D., Penberthy, W. T., Lin, S. and Zon, L. I. (2003). Transplantation and in vivo imaging of multilineage engraftment in zebrafish bloodless mutants. *Nat. Immunol.* **4**, 1238-1246.
Yamamoto, M. and Iuchi, I. (1975). Electron microscopic study of erythrocytes in developing rainbow trout, Salmo gairdnerii irideus, with particular reference to changes in the cell line. *J. Exp. Zool.* **191**, 407-426.
Zhang, Z.-W., Cheng, J., Xu, F., Chen, Y.-E., Du, J.-B., Yuan, M., Zhu, F., Xu, X.-C. and Yuan, S. (2011). Red blood cell extrudes nucleus and mitochondria against oxidative stress. *IUBMB Life* **63**, 560-565.

SUPPLEMENTAL INFORMATION

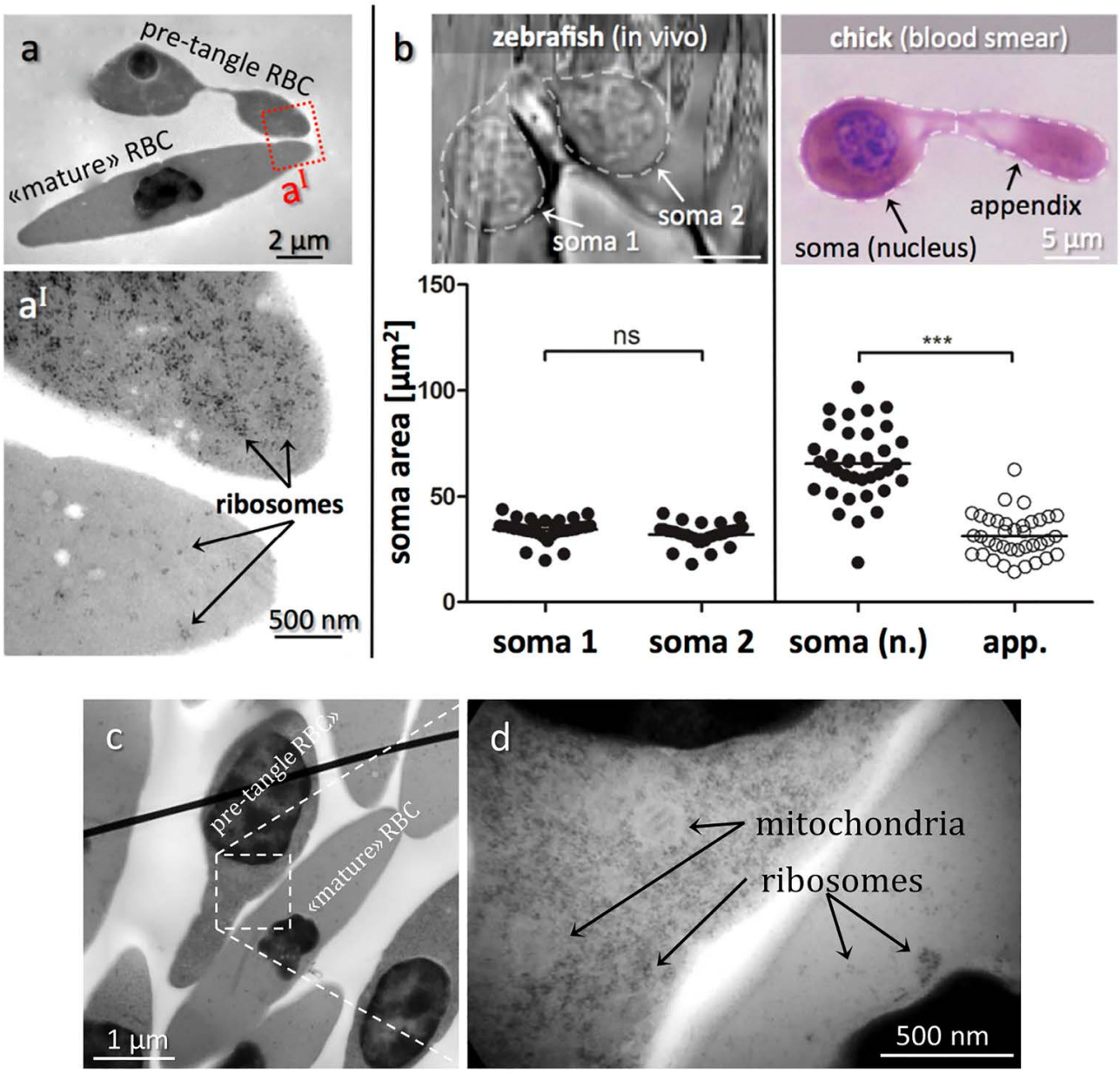

Fig. S1. Transmission electron micrographs of RBCs in blood of fish and chick embryos. (a) Electron micrographs comparing pre-tangle and mature chick RBCs. (a′) Zoomed region indicated in (a) in a pre-tangle RBC (top) contains abundant free ribosomes in contrast to the mature RBC (bottom). Other side-by-side comparisons of pre-tangling versus mature chick RBCs as shown in (c + d) confirmed the far higher quantity of ribosomes and mitochondria in immature RBCs relative to fully differentiated cells. (b) Comparing somata sizes of dumbbell-shaped zebrafish and chick RBCs. In the zebrafish, both somata are nucleated and of similar size. In contrast, only one soma is nucleated in the chick RBC, which is significantly larger in size than the other soma. ***P<0.001.

Movie 1. Formation of transluminal pillars and bifurcations. Time-lapse confocal imaging of the developing vasculature in the CVP of *Tg(fli1a:eGFP)* zebrafish between 28- 32 hpf. GFP-signal is represented in black. The vascular front rapidly expands by sprouting angiogenesis and joins to form the pole. Two arrows (red, green) indicate the appearance of two transluminal pillars. Such pillars are then integrated into the CVP and remain there for many hours or even days. They are the main site where *RBC splitting* occurs.

Movie 2. Exemplifying videos #1-4 of *RBC splitting* in the zebrafish embryo. RBCs are tangling up and splitting at a vascular pole. Time interval is indicated as min:sec. The videos were all captured between 39-45 hpf.

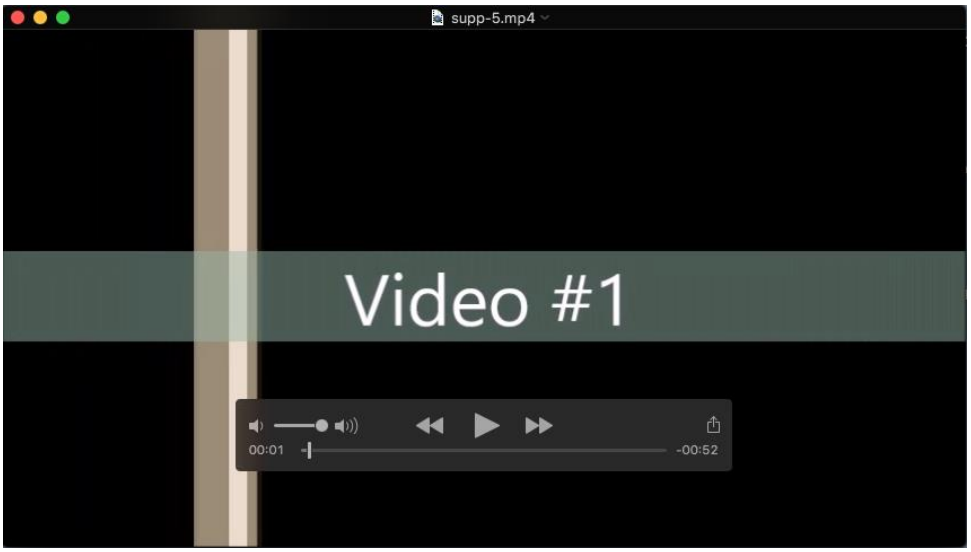

Movie 3. Examplifying videos #1-3 of tangled RBCs in the chicken chorioallantoic membrane (CAM) at d10. At day 10 after incubation (d10), the chick CAM contains high numbers of capillary beds. In these regions, dumbbell-shaped RBCs tangle up at vascular structures.